PHYSICAL REVIEW C **69**, 015801 (2004)

Solar neutrinos from CNO electron capture

L. C. Stonehill, J. A. Formaggio, and R. G. H. Robertson
Center for Experimental Nuclear Physics and Astrophysics, and Department of Physics, University of Washington, Seattle, Washington 98195, USA
(Received 23 September 2003; published 27 January 2004)

The neutrino flux from the sun is predicted to have a CNO-cycle contribution as well as the known *pp*-chain component. Previously, only the fluxes from β^+ decays of ^{13}N, ^{15}O, and ^{17}F have been calculated in detail. Another neutrino component that has not been widely considered is electron capture on these nuclei. We calculate the number of interactions in several solar neutrino detectors due to neutrinos from electron capture on ^{13}N, ^{15}O, and ^{17}F, within the context of the standard solar model. We also discuss possible nonstandard models where the CNO flux is increased.

DOI: 10.1103/PhysRevC.69.015801 PACS number(s): 23.40.−s, 26.65.+t, 14.60.Lm

I. INTRODUCTION

Experimental data gathered from both radiochemical [1–4] and real-time solar neutrino experiments [5,6] not only have revealed the phenomena of neutrino oscillations, but also have established the predominant mechanism for solar fuel burning [7]. The driving component for nuclear burning in the sun is the *pp* fusion chain. However, it is predicted that a portion of the solar neutrino flux also comes from the CNO cycle [8]. The CNO reaction products that have been shown to produce significant neutrino fluxes include β^+ decays of ^{13}N, ^{15}O, and ^{17}F. However, an additional source of neutrinos not previously evaluated in detail is electron capture on ^{13}N, ^{15}O, and ^{17}F. Electron capture produces a monoenergetic line spectrum with energy 1.022 MeV above the end point of the β^+ continuum. Bahcall [9] has considered electron capture from free electrons in the solar plasma, but not bound state electrons.

The increased sensitivity and precision of current and future solar neutrino experiments make it difficult to ignore contributions from these reactions. Moreover, the existence of a line spectrum presents an opportunity to make precision measurements of CNO fluxes. Existing solar neutrino experiments are sensitive to these neutrinos; in particular, the Sudbury Neutrino Observatory (SNO) is sensitive to the higher-energy CNO neutrinos produced from electron capture but not to the β^+ continuum. This contribution must be estimated in order to make a correct assessment of the ^{8}B flux—not only its magnitude, but also its spectral shape in the low-energy regime where matter effects are expected. In this paper, we calculate the predicted contribution to present and future solar neutrino experiments from CNO electron-capture neutrinos. In addition, we also discuss cases of nonstandard solar models in which the CNO flux is increased.

II. ELECTRON-CAPTURE FLUXES

The electron-capture processes that occur in the CNO cycle involve the following reactions:

$$^{13}\mathrm{N} + e^- \to {}^{13}\mathrm{C} + \nu_e, \tag{1}$$

$$^{15}\mathrm{O} + e^- \to {}^{15}\mathrm{N} + \nu_e, \tag{2}$$

$$^{17}\mathrm{F} + e^- \to {}^{17}\mathrm{O} + \nu_e. \tag{3}$$

If the electron-capture process is dominated by bound electrons, then it is possible to relate the electron-capture flux directly to the β^+ decay flux [10]. At solar temperatures and densities, however, one must take into account the contribution from both bound and continuum electrons. The ratio between electron-capture rates in the sun and laboratory measurements is given by [11]

$$R \equiv \frac{\lambda_{\mathrm{sun}}}{\lambda_{\mathrm{lab}}} = n_e \frac{|\psi(0)_{\mathrm{sun}}|^2}{2|\psi(0)_{\mathrm{lab}}|^2}, \tag{4}$$

where n_e is the electron density in the sun, and the atomic wave functions ψ are given by

$$|\psi(0)_{\mathrm{lab}}|^2 = \frac{1}{\pi} Z^3 \kappa(Z), \tag{5}$$

$$|\psi(0)_{\mathrm{sun}}|^2 = \exp\left(-\frac{Z\beta}{R_D}\right)(\omega_c + \omega_b). \tag{6}$$

Here Z is the charge, $\kappa(Z)$ is the correction term applied to the pure Coulomb field of $4Z^3\alpha^3$, as tabulated in Ref. [12], $\beta \equiv 1/kT$ is expressed in units of $\hbar = e = m_e = 1$ [13], and T is the solar temperature. The factors ω_c and ω_b are continuum and bound state electron density ratios at the nucleus for Coulomb-distorted waves relative to plane waves. Also included is a weak solar plasma screening correction which

TABLE I. The fraction of bound state electrons in the solar core, the atomic wave function at the nucleus in the sun, and the total correction to the electron-capture rate. Both fixed point (R_0) and volume-integrated (R_∞) ratios are shown. ^{7}Be is shown for comparison.

Element	$\omega_b/(\omega_c+\omega_b)$	$\lvert\psi(0)_{\mathrm{sun}}\rvert^2$	R_0	R_∞
^{7}Be	0.302	3.76	0.858	0.804
^{13}N	0.662	11.08	0.419	0.403
^{15}O	0.749	16.14	0.400	0.398
^{17}F	0.818	23.75	0.406	0.405

TABLE II. Neutrino fluxes from CNO electron capture. The final electron-capture flux takes into account the correction for capture of continuum electrons (R_∞). The CNO cycle is assumed to be at the level dictated by the SSM.

	SSM β^+ decay flux (cm^{-2} s^{-1})	$(EC/\beta^+ \text{ decay})_{lab}$	EC flux (cm^{-2} s^{-1})
^{13}N	$5.48\times10^8(^{+0.21\%}_{-0.17\%})$	1.96×10^{-3}	4.33×10^5
^{15}O	$4.80\times10^8(^{+0.25\%}_{-0.19\%})$	9.94×10^{-4}	1.90×10^5
^{17}F	$5.63\times10^6(^{+0.25\%}_{-0.25\%})$	1.45×10^{-3}	3.32×10^3

depends on the Debye radius R_D [14]. The continuum and bound state electron density ratios are given by [15]

$$\omega_c = \left\langle \frac{2\pi\eta}{1-e^{-2\pi\eta}} \right\rangle \tag{7}$$

$$\omega_b = \pi^{1/2}(2Z^2\beta)^{3/2} \sum \frac{1}{n^3} \exp\left(\frac{Z^2\beta}{2n^2}\right), \tag{8}$$

where $\eta = Z/v$ is the inverse velocity averaged over the electron Maxwell-Boltzmann distribution.

The electron density ratios are evaluated at both a fixed point in the solar core (R_0) and integrated over the entire solar volume (R_∞). The fixed point used is 0.057 of the solar radius, where the ^{13}N, ^{15}O, and ^{17}F fluxes peak. At this location, the temperature is 1.48×10^7 K, the Debye radius is 0.45, and the density is 5.32×10^{25} atoms/cm^3 [7]. The effect of the full integration on the fluxes is small for the nuclei of interest ($\sim$3% for ^{13}N and less than 1% for ^{15}O and ^{17}F). The total correction due to continuum electron capture is shown in Table I. The relative K-shell/L-shell occupancies for ^{13}N, ^{15}O, and ^{17}F are all greater than 90% [12]. Capture of both K- and L-shell electrons has been included here. For evaluation of the electron-capture rate with accuracy of a few percent the radiative corrections should be included (see, for example, Ref. [16]).

Table II shows the expected total rate of neutrinos from K shell and continuum electron-capture processes, assuming the solar burning cycle is dominated by *pp* fusion. The major contribution to the uncertainties on the electron-capture fluxes comes from the uncertainties on the standard solar model (SSM) β^+ decay fluxes [7]. The neutrino flux from these sources is of the same order as the ^8B flux, though at lower neutrino energies. The solar neutrino spectrum, including the CNO electron-capture neutrino lines, is shown in Fig. 1. There is in addition an electron-capture branch for ^8B decay [18], but its total flux is 1.3 cm^{-2} s^{-1}, too small to appear on the graph.

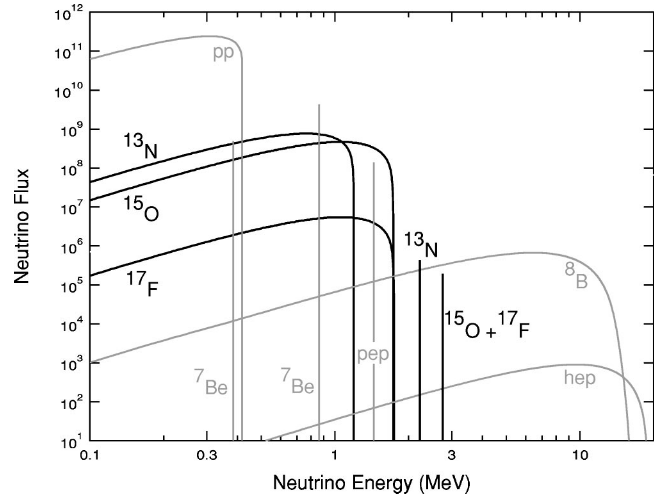

FIG. 1. Solar neutrino flux at 1 a.u., including electron capture in the CNO cycle. The *pp* chain is shown in gray and the CNO cycle is shown in black. Line fluxes are in cm^{-2} s^{-1} and spectral fluxes are in cm^{-2} s^{-1} MeV^{-1} The *pp* chain and the CNO β^+ decay fluxes are from Ref. [17].

To determine the observed rate at a given experiment, we consider charged current (CC), neutral current (NC), and elastic scattering (ES) interactions on a variety of targets. The cross sections used for ^2H, ^7Li, ^{37}Cl, and ^{71}Ga are taken from Refs. [19–22]. A precise accounting of radiative corrections has not yet been applied to all of these processes. In the case of deuterium targets, the value of $L_{1,A}$ [19] was set to 4.0 and radiative corrections are included [16]. For the elastic scattering cross section, the following relation was used:

$$\frac{d\sigma(\nu_e e^-)}{dT_e} = \frac{G_F^2 s}{\pi}\left\{g_L^2 + g_R^2\left(1-\frac{T_e}{E_\nu}\right)^2 - g_L g_R \frac{m_e T_e}{E_\nu^2}\right\}, \tag{9}$$

where G_F is the Fermi constant, s is the center-of-mass energy, $g_{L(R)}$ are the left (right) handed couplings for the weak current, T_e is the electron kinetic energy, and E_ν is the neutrino energy. Uncertainties on electron, ^2H, and ^7Li targets are well understood at the level of 1% [23]. Uncertainties in the CC cross sections for ^{37}Cl are dominated by transitions to forbidden states, which at these energies are 1–2%. For CC interactions on ^{71}Ga, allowed transitions to excited states play a significant role, and the uncertainties are expected to be larger at these energies. The expected neutrino rates for various targets are presented in Table

TABLE III. Neutrino interaction rates with various detector materials, assuming no neutrino oscillations. Rates are given in units of SNU's (1 SNU$\equiv10^{-36}$ interactions/atom/s), except for ES, which is given in 10^{-36} interactions/electron/s.

	Energy (MeV)	ES	^2H NC	^2H CC	^7Li	^{37}Cl	^{71}Ga
^{13}N	2.220	7.98×10^{-3}	0	3.63×10^{-3}	8.79×10^{-2}	2.11×10^{-3}	2.15×10^{-2}
^{15}O	2.754	4.46×10^{-3}	2.26×10^{-4}	5.79×10^{-3}	6.65×10^{-2}	1.60×10^{-3}	1.54×10^{-2}
^{17}F	2.761	7.80×10^{-5}	4.08×10^{-6}	1.02×10^{-4}	1.17×10^{-3}	2.80×10^{-5}	2.70×10^{-4}

TABLE IV. CNO electron-capture neutrino interaction rates in various detectors. Rates are presented for the SSM CNO fraction, the upper limit to the CNO fraction that comes from solar neutrino data, and a toy model where almost all of the solar luminosity is due to the CNO cycle. Rates are given as a fraction of the observed rate, except for BOREXINO, which is given as a fraction of the expected rate.

	SSM	7.3%	99.95%
SNO NC (salt phase)	0.01%	0.05%	0.6%
BOREXINO	0.1%	0.3%	4.3%
^{37}Cl	0.2%	0.7%	9.7%
^{71}Ga	0.1%	0.2%	3.3%

III. The relatively large rates suggest that a ^{7}Li-based detector might be a viable next-generation solar neutrino experiment. For example, a water Cherenkov detector with dissolved ^{7}Li, such as suggested in Ref. [24], might be a workable design.

Of particular interest is whether the CNO electron-capture flux constitutes a serious background for current neutrino experiments. For SNO, these NC rates correspond to about 0.4 ^{15}O neutrino NC event per year and about 0.01 ^{17}F events per year. The latter is negligible, but the ^{15}O contributes a small model-dependent background to the ^{8}B measurement. The CC interactions are below the SNO analysis threshold, so they do not contribute significantly to SNO results. Below the 5.5 MeV analysis threshold in the recent SNO publication [23] there were about 13 events expected from this source. The ES interactions could be detected in a liquid scintillator experiment such as KamLAND [25] or BOREXINO [26]. For example, in BOREXINO the electron-capture neutrino rates would be about 0.1% of the expected SSM signal. The expected rates for ^{71}Ga and ^{37}Cl have also been calculated and are shown in Table IV.

III. ALTERNATIVE SOLAR MODELS

This calculation has assumed that the CNO-cycle contribution to the solar luminosity is 1.5%, as predicted by the standard solar model [7]. That model is well established theoretically, and fits well with helioseismology data and the total ^{8}B solar neutrino flux measured by SNO. It is possible, however, to envision other solar models in which the CNO cycle is increased relative to the *pp* chain, while still fitting with available experimental data. For example, the authors of Ref. [27] suggested a model in which 99.95% of the solar energy comes from the CNO cycle while still agreeing with solar luminosity and the neutrino measurements to that date. In that model the ^{15}O β^{+} decay flux is 3.41×10^{10} cm^{-2} s^{-1}, a 70-fold increase over the SSM flux, which would raise the predicted ^{15}O electron-capture neutrino NC rate in SNO to 30 yr^{-1}. This increase in the CNO flux does not come at the expense of ^{8}B flux, as the ^{8}B flux in the model is 8.64×10^{6} cm^{-2} s^{-1}, even higher than the flux measured by SNO. The model was not proposed as a realistic solar model, rather it was an illustration of the possible level to which the CNO cycle could be raised in the sun.

Recent experimental results [1–6,25] constrain the fraction of energy that the sun produces via the CNO cycle to less than 7.3% at 3σ [28]. CNO electron-capture neutrino interaction rates in various neutrino detectors are shown in Table IV, in the context of the SSM as well as the 7.3% upper limit model and the 99.95% model. Future low-energy, high-resolution neutrino experiments can take advantage of the electron-capture channels to explicitly set more stringent limits on the fraction of CNO neutrinos.

IV. CONCLUSION

The neutrino flux from electron capture in the solar CNO cycle has been calculated. The rate of such neutrinos on current detectors is expected to be small, though the process does introduce a model-dependent background to the SNO measurement of the total ^{8}B flux, at the level of about one event per year. However, the model-dependence is small, since the fractional contribution of the CNO cycle to the solar luminosity is limited experimentally to 7.3%, only about a factor of 5 above the SSM fraction. Future experiments can take advantage of the monoenergetic nature of the neutrinos from electron capture to make a precision measurement of the fraction of the solar luminosity due to the CNO cycle.

ACKNOWLEDGMENTS

The authors would like to thank M. K. Bacrania for his assistance in preparing Fig. 1. This work was supported by the U.S. Department of Energy under Grant No. DE-FG06-90ER40537.

[1] B. T. Cleveland *et al.*, Astrophys. J. **496**, 505 (1998).
[2] J. N. Abdurashitov, J. Exp. Theor. Phys. **95**, 181 (2002); J. N. Abdurashitov *et al.*, Phys. Rev. C **60**, 055801 (1999).
[3] W. Hampel *et al.*, Phys. Lett. B **447**, 127 (1999).
[4] T. Kirsten, GNO Collaboration, Nucl. Phys. B, Proc. Suppl. **118**, 33 (2003).
[5] Q. R. Ahmad, SNO Collaboration, Phys. Rev. Lett. **89**, 011301 (2002).
[6] S. Fukuda *et al.*, Phys. Lett. B **539**, 179 (2002).
[7] J. N. Bahcall, M. H. Pinsonneault, and S. Basu, Astrophys. J. **555**, 990 (2001).
[8] H. A. Bethe, Phys. Rev. **55**, 434 (1939).
[9] J. N. Bahcall, Phys. Rev. D **41**, 2964 (1990).
[10] N. B. Gove and M. J. Martin, Nucl. Data Tables **10**, 3 (1971).
[11] I. Iben, K. Kalata, and J. Schwartz, Astrophys. J. **155**, 551 (1967).

[12] R. B. Firestone, *Table of Isotopes*, 8th ed. (Wiley, New York, 1996).
[13] With this convention, the unit of energy is the Hartree energy $m_e c^2 \alpha^2$ and the unit of length is the Bohr radius a_0.
[14] E. E. Salpeter, Aust. J. Phys. **7**, 373 (1954).
[15] A. V. Gruzinov and J. N. Bahcall, Astrophys. J. **490**, 437 (1997).
[16] A. Kurylov, M. J. Ramsey-Musolf, and P. Vogel, Phys. Rev. C **67**, 035502 (2003).
[17] See J. N. Bahcall, www.sns.ias.edu/~jnb/
[18] F. L. Villante, Phys. Lett. B **460**, 437 (1999).
[19] M. Butler, J.-W. Chen, and X. Kong, Phys. Rev. C **63**, 035501 (2001).
[20] J. N. Bahcall and E. Lisi, Phys. Rev. D **54**, 5417 (1996).
[21] J. N. Bahcall, Rev. Mod. Phys. **50**, 881 (1978).
[22] J. N. Bahcall *et al.*, Phys. Rev. C **54**, 411 (1996).
[23] S. N. Ahmed, SNO Collaboration nucl-ex/0309004.
[24] W. C. Haxton, Phys. Rev. Lett. **76**, 1562 (1996).
[25] K. Eguchi *et al.*, Phys. Rev. Lett. **90**, 021802 (2003).
[26] T. Schutt BOREXINO Collaboration, Nucl. Phys. B (Proc. Suppl.) **110**, 323 (2002).
[27] J. N. Bahcall, M. Fukugita, and P. I. Krastev, Phys. Lett. B **374**, 1 (1996).
[28] J. N. Bahcall, M. C. Gonzalez-Garcia, and C. Peña-Garay, Phys. Rev. Lett. **90**, 131301 (2003).